

pubs.acs.org/JPCA Article

Characterization of Competing Halogen- and Hydrogen-Bonding Motifs in Simple Mixed Dimers of HCN and HX (X = F, Cl, Br, and I)

Morgan A. Perkins and Gregory S. Tschumper*



Cite This: J. Phys. Chem. A 2022, 126, 3688-3695



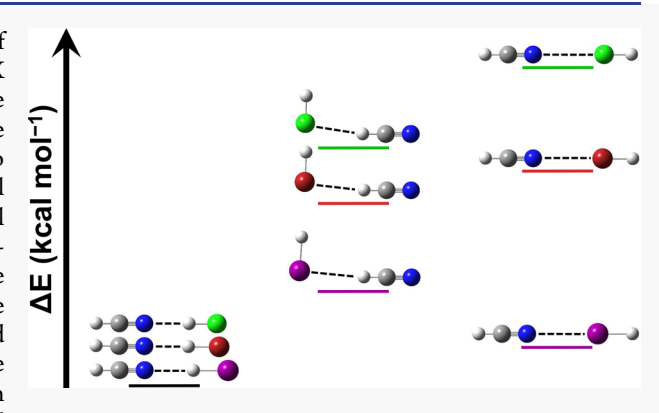
ACCESS I

Metrics & More

Article Recommendations

Supporting Information

ABSTRACT: This work performs the first systematic comparison of hydrogen- and halogen-bonded configurations of the HCN/HX mixed dimer, where X = F, Cl, Br, and I. Eleven different minima have been characterized for these four heterogeneous dimers near the CCSD(T) complete basis set (CBS) limit. For each complex, two different hydrogen-bonded minima were identified: the global minimum where HX acts as the hydrogen bond donor and a local minimum where HX acts as the hydrogen bond acceptor. A halogen-bonded local minimum was also identified for all but the fluorine mixed dimer. To the best of our knowledge, three of the minima are identified here for the first time. The hydrogen- and halogen-bonded local minima of each complex become more energetically competitive with the global minimum as the atomic radius of the halogen atom increases. CCSD(T) relative energies of the hydrogen-bonded local



minima computed near the CBS limit decrease from $4.5 \text{ kcal mol}^{-1}$ for HCN/HF to 2.9, 2.4, and $1.2 \text{ kcal mol}^{-1}$ for X = Cl, Br, and I, respectively. Corresponding relative energies for the halogen-bonded local minima range from $4.0 \text{ kcal mol}^{-1}$ for X = Cl to $2.7 \text{ kcal mol}^{-1}$ for X = Br and to as little as $0.5 \text{ kcal mol}^{-1} X = I$. Harmonic vibrational frequency shifts reported here suggest that it may be feasible to differentiate between the various minima for X = Cl, Br, and I via spectroscopic analysis, as was the case for the HCN/HF dimer.

INTRODUCTION

Studies on small molecular systems held together by weak intermolecular interactions can highlight the interplay of theory and experiment, since these types of systems can be amenable to both high-resolution gas-phase experimental study and high-accuracy computational analysis. 1,2 One such system that has been thoroughly characterized by both experimental $^{3-13}$ and computational $^{14-21}$ work is the hydrogen-bonded dimer of hydrogen cyanide (HCN) and hydrogen fluoride (HF). Two different hydrogen-bonded configurations of this mixed dimer have been identified experimentally (using rotational constants and H-F and C-H vibrational stretching frequencies) and characterized computationally: a linear structure with HF donating the hydrogen bond (HCN···HF, top of Figure 1) and a bent, planar structure where HF acts as the hydrogen bond (HB) acceptor (HF...HCN, bottom of Figure 1). Both structures are minima, but the linear structure is signficantly lower in energy (by approximately 5 kcal mol⁻¹)^{16,21} and therefore will be referred to as the hydrogenbonded global minimum (GM_{HB}) while the bent HF···HCN will be referred to as the hydrogen-bonded local minimum (LM_{HB}). A recent computational study also identified a planar transition state that indicated an electronic barrier of \approx 0.5 kcal mol⁻¹ exists for in-plane rearrangement of the HB topology from LM_{HB} to GM_{HB} (HF···HCN \rightarrow HCN···HF).²¹ In the



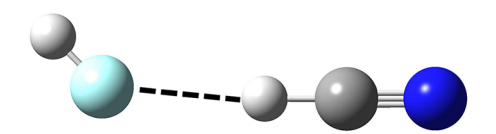


Figure 1. Linear global (top) and bent local (bottom) hydrogen-bonded minima of the heterogeneous HCN/HF dimer denoted GM_{HB} and LM_{HB} , respectively.

same study, MP2 and CCSD(T) computations were able to accurately reproduce experimental properties such as funda-

Received: March 24, 2022 Revised: May 7, 2022 Published: June 2, 2022





mental vibrational frequencies, the dissociation energy, and the length of the HB.

Other hydrogen halides can also participate in analogous HB interactions with HCN. The linear HCN···HX configuration in which the hydrogen halide is the HB donor has been detected in the gas phase for X = Cl, Br, and I^{22-31} and has also been characterized in a number of computational studies using quantum mechanical electronic structure techniques and other theoretical models. To the best of our knowledge, the reversed HB arrangement where HCN is the HB donor (i.e., the HX···HCN configuration) has not been observed experimentally for X = Cl, Br, or I, and it has only been studied computationally for X = Cl.

In addition to participating in hydrogen-bonding interactions, the heavier halides (Cl, Br, and I) are also known to form halogen bonds (XB): attractive interactions between the electrophilic region, or σ -hole, of a halogen atom and a nucleophile.⁵³ Nitrogen is a common XB acceptor, and a few computational studies have reported linear, halogen-bonded configurations of the form HCN···XH for X = Br and $I.^{54-56}$ Studies of the HCN/HX heterogeneous dimer focus exclusively on either the HB or the XB configurations, and to date no studies have looked more broadly at both possiblilities for these systems. Both halogen and hydrogen bonds are important to many fields, such as supramolecular chemistry and biochemistry, and extensive research has been done to investigate the relationship between these two noncovalent interactions. 57-63 Taking a look at how they compete in a relatively simple dimer system that is both computationally and experimentally accessible can give researchers insight into their roles in more complex systems. This study will provide the first systematic investigation of the different HB and XB topologies in this series of HCN/HX mixed dimers (X = F, Cl, Br, and I). Properties related to the formation of the intermolecular bond, such as dissociation energy and vibrational frequency shifts, will be compared across the entire series.

■ COMPUTATIONAL DETAILS

The dimer configurations of HCN/HX (X = F, Cl, Br, and I) and their associated monomers were fully optimized using both MP2⁶⁴ and CCSD(T)^{65–67} with a series of correlation consistent basis sets augmented with diffuse functions on all atoms except hydrogen, i.e., cc-pVYZ for H; aug-cc-pVYZ for F, C, N, Cl, and Br; and aug-cc-pVYZ-PP for I (which includes a relativistic pseudopotential used for the 28 core electrons of all I atoms). $^{68-74}$ All basis sets are denoted heavy-aug-cc-pVYZ or haYZ, where Y = T, Q, and 5. Harmonic vibrational frequency computations were used to characterize each stationary point as either a minimum, transition state, or higher-order saddle point using the same series of methods and basis sets.

Gaussian16⁷⁵ was used for all MP2 computations and CFOUR⁷⁶ was used for all CCSD(T) computations. Gradients were computed analytically for all geometry optimizations. Hessians were computed analytically for all MP2 computations and for all CCSD(T) computations that did not contain iodine. CCSD(T) Hessians for all iodine-containing systems were computed numerically from finite differences of analytic gradients. The frozen-core approximation was used for all computations, excluding from the correlation procedure the two core electrons of C, N, and F, the ten core electrons of Cl, and the 18 core electrons of Br. For I, 28 core electrons were

replaced by the 28MDF pseudopotential and 8 more electrons were excluded from the correlation procedure (following the default frozen-core approximation in Gaussian16 for aug-cc-pVYZ-PP on I). Additional MP2 computations were carried out on select systems containing Br and I to examine the effects of using pseudopotentials and different frozen-core approximations. The results have been relegated to the Supporting Information because they did not significantly affect the properties reported in this study.

Dissociation energies were computed for each system's global minimum. Computing electronic dissociation energies using finite basis sets gives rise to an inconsistency known as basis set superposition error (BSSE). In order to assess the effect of BSSE on the systems examined here, the counterpoise procedure $(CP)^{79-81}$ was employed, following the procedure outlined elsewhere.

RESULTS

HCN/HX Structures. For each HCN/HX mixed dimer (X = F, Cl, Br, and I), two different hydrogen-bonded minima were identified: the linear global minimum (GM) where HX donates the HB (HCN···HX, labeled GM_{HB}) and a nonlinear local minimum (LM) where HX becomes the HB acceptor (HX···HCN, labeled LM_{HB}). For the heavier halides (X = Cl, Br, and I), a linear, halogen-bonded minimum was identified (HCN···XH, labeled LM_{XB}). An analogous LM_{XB} stationary point could not be identified for the HCN/HF dimer, which is to be expected, as it is generally accepted that fluorine does not participate in halogen bonding in the same manner as Cl, Br, and I. This is due to fundamental differences in the underlying noncovalent interactions, though the specifics of those differences are to some extent dependent on the criteria used to define a halogen bond. 83-89 All three minima are depicted for each halide in Figure 2: a schematic of CCSD(T)/ha5Z relative electronic energies (ΔE) for the minima with respect to each complex's own GM. Table 1 contains the HB or XB length for each structure and, specifically for LM_{HB}, two

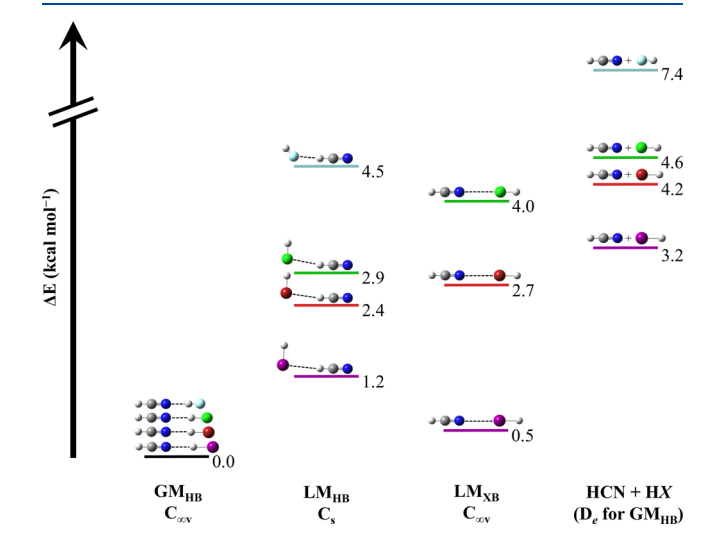


Figure 2. CCSD(T)/ha5Z relative electronic energies for the HCN/HX dimer minima and dissociation energies of the global minima (rightmost column) for X = F (light blue), Cl (green), Br (red), and I (purple). In each column, the energetic ordering (from the bottom to the top) consistently remains I < Br < Cl < F, with the exception of LM_{XB} , which has no equivalent configuration for X = F.

Table 1. Selected CCSD(T)/ha5Z Intermolecular Bond Lengths (r in Å) and Angles $(\theta \text{ in degrees})$ for the HCN/HX Minima

	GM_{HB}	$LM_{ m HB}$			LM_{XB}
	r(N···H)	$r(X \cdots H)$	$\theta(HX\cdots H)$	$\theta(X \cdots HC)$	$r(N\cdots X)$
F^a	1.85	2.13	139	176	N/A
Cl	2.08	2.70	99	170	3.30
Br	2.12	2.83	95	172	3.24
I	2.25	3.03	92	175	3.26
^a Ref 2	1.				

intermolecular angles that help quantify deviations from linearity. The LM_{XB} stationary point for X=Cl is identified in this work for the first time, along with the LM_{HB} stationary points for the bromine and iodine dimers. The majority of the data presented for the fluorine complexes and monomers was taken directly from ref 21, which performed similar computations using the same methods and basis sets employed in this work. The only new data presented here for HCN/HF comes from a single harmonic vibrational frequency computation that was run at the CCSD(T)/ha5Z level of theory for the LM_{HB} configuration.

For the GM_{HB} configurations (left side of Table 1), the HB distance increases with the atomic radius of the halogen atom (F < Cl < Br < I), from 1.85 Å for HCN···HF to 2.25 Å for HCN···HI. This trend for the computed HB length is consistent with the experimental N···X distances of 2.8043 Å for F, 3.4047 Å for Cl, 23 3.6104 Å for Br, 25 and 3.9129 Å for I,²⁹ inferred from rotational parameters and rigid geometries of the isolated monomers. The computed N···X separations (tabulated in the Supporting Information for each level of theory) are always within 0.1 Å of the corresponding experimental data for the CCSD(T) structures, regardless of the basis set used in the optimization. As with GM_{HB} , the HB distance for LM_{HB} (center of Table 1) increases with increasing halogen size, going from 2.13 Å for the F analogue to 3.03 Å for the I analogue. For each halogen, the HB distance is at least 0.3 Å larger for the LM_{HB} configuration than for the corresponding GM_{HB}. The halogen atom is nearly colinear with HCN in the LM_{HB} configuration. The X···HC angle falls between 170° and 176° degrees for each CCSD(T)/ha5Z structure. In contrast, the HX···H angle is appreciably smaller and indicates significant deviations from linearity. $\theta(HX\cdots H)$ is 139° for X = F, and it decreases to 99°, 95°, and 92° for X = Cl, Br, and I, respectively. The XB distances for the LM_{XB} structures are all similar to one another. The Cl analogue has the longest XB at 3.30 Å, and Br and I have halogen bonds of similar length: 3.24 and 3.26 Å, respectively.

The HCN and HX monomers undergo some structural changes upon complexation. Table 2 details the most significant changes in intramonomer bond length (Δr) for all three dimer minima at the CCSD(T)/ha5Z level of theory. Any changes that exceeded ± 0.001 Å for at least one of the minima are listed. The largest deformations were observed for the HX bonds in the GM_{HB} configuration, where $\Delta r(\text{HX})$ consistently increased from +0.005 Å for HI to +0.012 Å for HF. These GM_{HB} minima also exhibited a much smaller contraction of the CN bond in HCN that increased from $\Delta r(\text{CN}) = -0.001$ Å for the iodine complex to $\Delta r(\text{CN}) = -0.003$ Å for the fluorine complex. All bond length changes were appreciably small for the LM_{HB} minima, where HX plays the role of the HB acceptor. $\Delta r(\text{HX})$ is only +0.001 or +0.002

Table 2. CCSD(T)/ha5Z Intramolecular Bond Length Changes (Δr in Å) upon Complexation That Exceed ± 0.001 Å for the HCN/HX Minima

	GM_{HB}		LM_{HB}		LM_{XB}
	$\Delta r(\mathrm{HX})$	$\Delta r(\mathrm{CN})$	$\Delta r(\mathrm{HX})$	$\Delta r(HC)$	$\Delta r(HX)$
F^a	+0.012	-0.003	+0.002	+0.003	N/A
Cl	+0.010	-0.002	+0.001	+0.002	+0.000
Br	+0.008	-0.002	+0.001	+0.003	+0.002
I	+0.005	-0.001	+0.001	+0.003	+0.005
^a Ref 21					

Å, and the change to the donor CH bond length is only slightly larger, with $\Delta r(\text{HC})$ values of either +0.002 or +0.003 Å. For the halogen-bonded minima, only the HBr and HI bonds changed by more than ± 0.001 Å ($\Delta r(\text{HX}) = +0.002$ and +0.005 Å, respectively). CCSD(T)/haYZ Cartesian coordinates and selected geometrical parameters of the CCSD(T)/ha5Z optimized structures are provided in the Supporting Information for each minimum and the isolated monomers.

While searching for minima, additional stationary points with one or more imaginary frequencies $(n_i \ge 1)$ were identified for each HCN/HX dimer. A planar transition state analogous to that identified previously for X = F was identified for X = Cl, Br, and I (labeled TS1 in the Supporting Information). A second planar transition state, labeled TS2, was also identified for the larger halides (X = Br and I). The C_s structures of TS1 and TS2 are depicted in Figure S1 along with selected optimized intermolecular geometrical parameters (Table S3) and relative electronic energies with respect to GM_{HR} (Tables S4 and S5).

TS1 was previously reported as a transition state for HCN/HF that connects LM_{HB} to GM_{HB} through an in-plane pathway. For HCN/HF, electronic energies computed near the CCSD(T) CBS limit indicate that TS1 provides a barrier of approximately 0.5 kcal mol⁻¹ for the in-plane pathway, along which LM_{HB} collapses to GM_{HB} (HF···HCN \rightarrow HCN···HF). Although that barrier is sufficiently large to enable experimental identification of both hydrogen-bonded structures when $X = F_{i}^{6,16}$ the corresponding electronic barrier height decreases substantially for Cl, Br, and I (\leq 0.2 kcal mol⁻¹).

The second planar transition state has been identified for the Br and I systems. TS2 likely represents the barrier for the rearrangement between the halogen-bonded and hydrogenbonded structures along a planar pathway. This tentative designation is consistent with the normal-mode displacements associated with the imaginary vibrational frequency of TS2, as well as the absence of this stationary point for the HCN/HF system, which does not have a halogen-bonded minimum. For Br, TS2 lies only ca. 0.3 kcal mol⁻¹ above LM_{XB} near the CCSD(T) CBS limit. This barrier along the planar pathway between the XB and HB structures increases to more than 1 kcal mol^{-1} for X = I. If there are not any other lower-energy planar or nonplanar pathways for this rearrangement in the HCN/HI dimer then it is likely that both the hydrogenbonded global minimum and the halogen-bonded local minimum can be detected experimentally under appropriate conditions. However, an exhaustive search for other rearrangement mechanisms with robust ab initio methods lies beyond the scope of this investigation.

An additional linear HX···HCN stationary point was identified for all four halides via MP2 optimizations, and all

were found to be higher-order saddle points $(n_i \ge 2)$. As such, additional CCSD(T) computations were not performed on these relatively high-energy structures. The MP2/haYZ energetics and Cartesian coordinates for these stationary points and the other structures (GM_{HB}, LM_{HB}, LM_{XB}, TS1, TS2) are reported in the Supporting Information.

HCN/HX Energetics. The CCSD(T) relative electronic energies for all of the minima are given in Table 3, along with

Table 3. CCSD(T) Relative Electronic Energies in kcal mol^{-1} of the Hydrogen- and Halogen-Bonded Minima for the HCN/HX Dimers As Well As the Electronic Dissociation Energy for the Global Minimum, with and without ZPVE Corrections (D_0 and D_e , Respectively, in kcal mol^{-1})

	GM_{HB}	LM_{HB}	LM_{XB}	D_e	D_0
			F^a		
haTZ	0.00	4.60	N/A	7.63	5.58
haQZ	0.00	4.55	N/A	7.52	5.49
ha5Z	0.00	4.48	N/A	7.43	5.44
			Cl		
haTZ	0.00	2.96	3.93	4.72	3.35
haQZ	0.00	2.92	3.98	4.67	3.33
ha5Z	0.00	2.87	3.95	4.61	3.32
			Br		
haTZ	0.00	2.42	2.51	4.33	3.06
haQZ	0.00	2.32	2.59	4.24	3.07
ha5Z	0.00	2.36	2.66	4.20	3.01
			I		
haTZ	0.00	1.44	0.32	3.26	2.23
haQZ	0.00	1.37	0.33	3.26	2.32
ha5Z	0.00	1.23	0.46	3.20	2.28
^a Ref 21.					

the electronic dissociation energy with and without harmonic zero-point vibrational energy (ZPVE) corrections (D_0 and D_{el} respectively) for the GM of each dimer. A larger D_e corresponds to a stronger HB, and the HB strength decreases with increasing halogen size. The D_c ranges from ca. 7.4 kcal mol⁻¹ for HCN···HF to ca. 3.2 kcal mol⁻¹ for HCN···HI at the CCSD(T)/ha5Z level of theory. The decrease in D_e is the largest when moving from the fluorine to the chlorine dimer. Dissociation energies with the CP procedure applied (D_e^{CP}) are tabulated in the Supporting Information. For the smaller halogens (fluorine and chlorine), D_e and D_e^{CP} differ by no more than 0.1 kcal mol⁻¹ at both the MP2 and CCSD(T) level of theory using the ha5Z basis set. For bromine and iodine, the two D_e values differ by no more than 0.5 kcal mol⁻¹ at the MP2/ha5Z level of theory and 0.4 kcal mol⁻¹ at the CCSD(T)/ha5Z level of theory. As expected, including ZPVE decreases the magnitude of the dissociation energy $(D_0 < D_e)$, though the overall trend of decreasing bond strength stays the same. D_0 ranges from ca. 5.4 kcal mol⁻¹ for HCN···HF to 2.3 kcal mol⁻¹ for HCN···HI at the CCSD(T)/ ha5Z level of theory. MP2 consistently overestimates both D_e and D_0 for each mixed dimer, regardless of basis set size (values tabulated in the Supporting Information).

Both of the local minima (LM_{HB} and LM_{XB}) become more energetically competitive with the GM as the size of the halogen atom increases. The fluorine LM_{HB} , which has been detected experimentally, lies 4.5 kcal mol⁻¹ above the corresponding global minimum, according to CCSD(T)/T

ha5Z electronic energies. That difference decreases to 2.9, 2.4, and 1.2 kcal mol $^{-1}$ for the chlorine, bromine, and iodine analogues, respectively. The ΔE of the halogen-bonded minimum at the CCSD(T)/ha5Z level of theory decreases from 4.0 kcal mol $^{-1}$ for Cl to 2.7 kcal mol $^{-1}$ for Br and to only 0.5 kcal mol $^{-1}$ for I. CCSD(T) ΔE values with the ZPVE correction applied are tabulated in the Supporting Information. The ZPVE corrected values are smaller than the noncorrected values, up to 1.4 kcal mol $^{-1}$ lower for the LM $_{\rm HB}$ minima and 0.7 kcal mol $^{-1}$ lower for the LM $_{\rm XB}$ minima. Most importantly, including ZPVE does not change the relative energetic ordering of any of the minima. The MP2 ΔE values are never more than 0.5 kcal mol $^{-1}$ above their corresponding CCSD(T) energies.

Vibrational Frequencies of the HCN/HX Minima. The CCSD(T) hydrogen halide harmonic vibrational stretching frequencies ($\omega_{\rm HX}$) are presented for each isolated HX molecule in Table 4. These stretching frequencies are shifted ($\Delta\omega_{\rm HX}$)

Table 4. CCSD(T) Harmonic StretcHing Frequencies of the Isolated HX Monomers and the Corresponding Frequency Shifts ($\omega_{\rm HX}$ and $\Delta\omega_{\rm HX}$, Respectively, in cm⁻¹) Induced by Hydrogen or Halogen Bonding in the Different Dimer Minima

	haTZ	haQZ	ha5Z	
		$\omega_{ ext{HX}}$		
F^a	4126	4142	4143	
Cl	2989	2990	2995	
Br	2685	2678	2673	
I	2338	2377	2328	
		$\Delta\omega_{ m HX}~({ m GM}_{ m HB})$		
F^a	-247	-255	-254	
Cl	-112	-123	-124	
Br	-70	-88	-87	
I	-23	-34	-37	
		$\Delta\omega_{ m HX}~({ m LM}_{ m HB})$		
F	-22^{a}	-21^{a}	-21	
Cl	-11	-12	-12	
Br	-8	-7	-9	
I	-4	-5	-5	
		$\Delta \omega_{ m HX} \; ({ m LM}_{ m XB})$		
F	N/A	N/A	N/A	
Cl	-4	-4	-4	
Br	-11	-12	-12	
I	-15	-18	-26	
^a Ref 21.				

upon formation of the mixed dimer as a result of the formation of either a HB (for GM_{HB} and LM_{HB}) or a XB (for LM_{XB}). The $\Delta\omega_{HX}$ values are well-converged at the CCSD(T)/ha5Z level of theory with the haQZ and ha5Z frequency shifts presented in Table 4 differing by no more than 8 cm⁻¹ for the LM_{XB} configuration of the HCN/HI dimer and by no more than 3 cm⁻¹ in every other case. Although the CCSD(T)/haQZ vibrational frequency is anomalously large for the HI stretching frequencies, the discrepancy vanishes when the corresponding core—valence quadruple- ζ correlation consistent basis set ⁹⁰ for I is adopted without the use of the frozen-core approximation for MP2 (details in the Supporting Information).

For GM_{HB} at the CCSD(T)/ha5Z level of theory, the fluorine system undergoes the largest frequency shift upon complexation ($\Delta\omega_{\rm HF} = -254~{\rm cm}^{-1}$). The magnitude of the

shifts decreases with increasing hydrogen bond length, down to a value of $-37~{\rm cm}^{-1}$ for $\Delta\omega_{\rm HI}.$ Shifts for the LM stationary points (LM $_{\rm HB}$ and LM $_{\rm XB}$) are not as large as the shifts for GM $_{\rm HB}.$ The LM $_{\rm HB}$ configuration's largest CCSD(T)/ha5Z frequency shift is only $-21~{\rm cm}^{-1}$ for the fluorine minimum and decreases to as little as $-5~{\rm cm}^{-1}$ for the iodine analogue. The shifts follow the opposite trend for the LM $_{\rm XB}$ configuration, increasing from $\Delta\omega_{\rm HCI}=-4~{\rm cm}^{-1}$ to $\Delta\omega_{\rm HI}=-26~{\rm cm}^{-1}.$

The HC stretches ($\omega_{\rm HC}$) in each LM_{HB} structure have the only other pronounced shifts associated with the harmonic vibrational frequencies of the three minima. For all of the LM_{HB} stationary points, the HC frequency shifts ($\Delta\omega_{\rm HC}$) are very well converged at the CCSD(T)/ha5Z level of theory, changing by no more than 3 cm⁻¹ from the CCSD(T)/haQZ values. The frequency shifts are all in a range from -29 to -39 cm⁻¹ at the CCSD(T)/ha5Z level of theory, increasing only moderately from the fluorine to the iodine dimer. The HC stretch for the HCN monomer and corresponding frequency shifts in the dimers are tabulated in the Supporting Information.

Although these results are based on harmonic vibrational frequency computations, the shifts discussed here and the IR intensities in the Supporting Information do suggest that it may be feasible to spectroscopically differentiate between the various minima for X = Cl, Br, and I, as was the case for the HCN/HF dimer. The CCSD(T) vibrational stretching frequencies and corresponding IR intensities for the monomers and dimer minima are reported in the Supporting Information, along with equivalent MP2 data. MP2 overestimates all frequency shifts for the mixed halide dimers, by as much as $60~{\rm cm}^{-1}$ for $\Delta\omega_{\rm HX}$ and $9~{\rm cm}^{-1}$ for $\Delta\omega_{\rm HC}$.

CONCLUSIONS

Three different minima on the potential energy surface of the HCN/HX dimer (X = Cl, Br, I) have been examined with CCSD(T) near the complete basis set (CBS) limit. Two HCN/HF minima characterized by a previous computational study²¹ are also included in the examination. For each halide, two hydrogen-bonded minima analogous to those identified experimentally for the HCN/HF dimer¹⁶ (Figure 1) were characterized: the global minimum where HX donates the hydrogen bond (HCN···HX) and a nonlinear local minimum where HX becomes the hydrogen bond acceptor (HX···HCN). A halogen-bonded minimum (HCN···XH) was also identified for X = Cl, Br, and I but not for X = F.

The hydrogen-bonded HX···HCN local minima are more energetically competitive for X = Cl, Br, and I ($\Delta E = 2.9, 2.4$, and 1.2 kcal mol⁻¹, respectively) than for X = F (ΔE = 4.5 kcal mol^{-1}). For X = Br and I, the halogen-bonded local minima, LM_{XB}, have relative electronic energies on par with the LM_{HB} structure ($\Delta E = 2.7 \text{ kcal mol}^{-1} \text{ for Br}$) and even with the GM_{HB} structure ($\Delta E = 0.5 \text{ kcal mol}^{-1}$ for I). Given that both the hydrogen- and halogen-bonded local minima for the chlorine, bromine, and iodine halides are relatively close in energy to their respective GM, it is possible that they could be identified experimentally. Vibrational frequency shifts for the HX and HC stretches upon dimer formation are presented for the different minima of each halide, and the IR intensities and harmonic frequency shifts provide potential guides for experimentally differentiating between the minima. Since formation of the minima will also depend on energetic barriers to move between the different structures, a more in-depth analysis of the low-energy pathways connecting the different

minima would be a beneficial extension of this work. A subsequent anharmonic treatment of the vibrational frequencies for the minima would also be beneficial and aid in the experimental interrogation of these small binary complexes.

ASSOCIATED CONTENT

Supporting Information

The Supporting Information is available free of charge at https://pubs.acs.org/doi/10.1021/acs.jpca.2c02041.

Additional geometrical parameters, energetic data, harmonic vibrational frequencies and corresponding IR intensities, and Cartesian coordinates (PDF)

AUTHOR INFORMATION

Corresponding Author

Gregory S. Tschumper — Department of Chemistry and Biochemistry, University of Mississippi, University, Mississippi 38677-1848, United States; Orcid.org/0000-0002-3933-2200; Email: tschumpr@olemiss.edu

Author

Morgan A. Perkins – Department of Chemistry and Biochemistry, University of Mississippi, University, Mississippi 38677-1848, United States; occid.org/0000-0002-6496-2335

Complete contact information is available at: https://pubs.acs.org/10.1021/acs.jpca.2c02041

Notes

The authors declare no competing financial interest.

ACKNOWLEDGMENTS

This work was supported in part by the National Science Foundation (CHE-1664998 and CHE-1757888). The Mississippi Center for Supercomputing Research (MCSR) is also thanked for a generous allocation of time on their computational resources.

REFERENCES

- (1) Chałasiński, G.; Gutowski, M. Weak interactions between small systems. Models for studying the nature of intermolecular forces and challenging problems for ab initio calculations. *Chem. Rev.* **1988**, 88, 943–962.
- (2) Mata, R. A.; Suhm, M. A. Benchmarking Quantum Chemical Methods: Are We Heading in the Right Direction? *Angew. Chem., Int. Ed.* **2017**, *56*, 11011–11018.
- (3) Thomas, R. K. Hydrogen Bonding in the Gas Phase: The Infrared Spectra of Complexes of Hydrogen Fluoride with Hydrogen Cyanide and Methyl Cyanide. *Proc. R. Soc. London A* **1971**, 325, 133–149.
- (4) Legon, A. C.; Millen, D. J.; Rogers, S. C. Dipole Moment Enhancement on Formation of a Hydrogen-bonded Complex. Demonstration and Measurement of the Effect for HCN···HF by Microwave Spectroscopy. *Chem. Phys. Lett.* **1976**, *41*, 137–138.
- (5) Legon, A. C.; Millen, D. J.; Rogers, S. C. The Electric Dipole Moment of the Hydrogen-bonded Heterodimer HCN···HF. An Investigation of the Conditions Leading to Inadequacy of the Secondand Fourth-Order Perturbation Theories of the Stark Effect for Linear Molecules. *J. Mol. Spectrosc.* 1978, 70, 209–215.
- (6) Andrews, L.; Johnson, G. L. FTIR Spectra of Water-Hydrogen Fluoride Complexes in Solid Argon. Evidence for Inversion Doubling in the HF Librational Modes of H₂O···HF. *J. Chem. Phys.* **1983**, *79*, 3670–3677.

- (7) Gallegos, A. M.; Rogers, B.; McMillan, K.; Shoja-Chaghervand, P.; Rodgers, A. S.; Bevan, J. W. Investigations Involving Near Infrared Rovibrational Spectra Observed in Gas-phase Linear Hydrogenbonded Complexes. Spectroscopy (Amsterdam, Neth.). 1983, 2, 62–68.
- (8) Wofford, B. A.; Bevan, J. W.; Olson, W. B.; Lafferty, W. J. Rovibrational analysis of ν_3 HCN-HF using Fourier transform infrared spectroscopy. *J. Chem. Phys.* **1985**, 83, 6188–6192.
- (9) Legon, A. C.; Millen, D. J.; Willoughby, L. C. Spectroscopic investigations of hydrogen bonding interactions in the gas phase. X. Properties of the hydrogen-bonded heterodimer HCN···HF determined from hyperfine coupling and centrifugal distortion effects in its ground-state rotational spectrum. *Proc. R. Soc. London A* 1985, 401, 327–347.
- (10) Legon, A. C.; Millen, D. J. Gas-Phase Spectroscopy and the Properties of Hydrogen-Bonded Dimers: HCN···HF as the Spectroscopic Prototype. *Chem. Rev.* **1986**, *86*, 635–657.
- (11) Wofford, B. A.; Bevan, J. W.; Olson, W. R.; Lafferty, W. J. Rovibrational Analysis of the $\nu_1{}^5$ Band in the HCN–HF Hydrogen Bonded Cluster. *Chem. Phys. Lett.* **1986**, 124, 579–582.
- (12) Wofford, B. A.; Jackson, M. W.; Bevan, J. W.; Olson, W. B.; Lafferty, W. J. Rovibrational analysis of an intermolecular hydrogen-bonded vibration: The ν_6^1 band of HCN–HF. *J. Chem. Phys.* **1986**, 84, 6115–6118.
- (13) Bender, D.; Eliades, M.; Danzeiser, D. A.; Jackson, M. W.; Bevan, J. W. The gas phase infrared spectrum of ν_1 and ν_1 - ν_4 HCN–HF. *J. Chem. Phys.* **1987**, *86*, 1225–1234.
- (14) Johansson, A.; Kollman, P.; Rothenberg, S. Hydrogen Bonding and the Structure of the HF-HCN Dimer. *Chem. Phys. Lett.* **1972**, *16*, 123–127.
- (15) Gadre, S. R.; Bhadane, P. K. Patterns in hydrogen bonding via electrostatic potential topography. *J. Chem. Phys.* **1997**, *107*, 5625–5626.
- (16) Douberly, G. E.; Miller, R. E. The Isomers of HF-HCN Formed in Helium Nanodroplets: Infrared Spectroscopy and *ab initio* Calculations. *J. Chem. Phys.* **2005**, *122*, 024306.
- (17) Domagala, M.; Grabowski, S. J. $X-H\cdots\pi$ and $X-H\cdots N$ Hydrogen Bonds Acetylene and Hydrogen Cyanide as Proton Acceptor. *Chem. Phys.* **2009**, *363*, 42–48.
- (18) Boese, A. D. Assessment of Coupled Cluster Theory and more Approximate Methods for Hydrogen Bonded Systems. *J. Chem. Theory Comput.* **2013**, *9*, 4403–4413.
- (19) Terrabuio, L. A.; Richter, W. E.; Silva, A. F.; Bruns, R. E.; Haiduke, R. L. A. An Atom in Molecules Study of Infrared Intensity Enhancements in Fundamental Donor Stretching Bands in Hydrogen Bond Formation. *Phys. Chem. Chem. Phys.* **2014**, *16*, 24920.
- (20) Rivera-Rivera, L. A.; Hren, Z. R. Compound-model morphed potential for the hydrogen bond HCN···HF. *Mol. Phys.* **2019**, *117*, 539–546.
- (21) Sexton, T. M.; van Benschoten, W. Z.; Tschumper, G. S. Dissociation energy of the HCN···HF dimer. *Chem. Phys. Lett.* **2020**, 748, 137382.
- (22) Thomas, R. K.; Thompson, H. W. Hydrogen bonding in the vapour phase: an unusual type of infrared band. *Proc. R. Soc. London A* **1970**, *316*, 303–313.
- (23) Legon, A. C.; Campbell, E. J.; Flygare, W. H. The rotational spectrum and molecular properties of a hydrogen-bonded complex formed between hydrogen cyanide and hydrogen chloride. *J. Chem. Phys.* **1982**, *76*, 2267–2274.
- (24) Legon, A. C.; Millen, D. J. Determination of properties of hydrogen-bonded dimers by rotational spectroscopy and a class-fication of dimer geometries. *Faraday Discuss. Chem. Soc.* **1982**, 73, 71–87.
- (25) Campbell, E. J.; Legon, A. C.; Flygare, W. H. The rotational spectrum and molecular properties of the hydrogen cyanide hydrogen bromide complex. *J. Chem. Phys.* **1983**, *78*, 3494–3500.
- (26) Bender, D.; Eliades, M.; Danzeiser, D.; Fry, E.; Bevan, J. Gasphase rovibrational analysis of ν_1 HCN-H³⁵Cl. *Chem. Phys. Lett.* **1986**, 131, 134–139.

- (27) Legon, A. C. In Structure and Dynamics of Weakly Bound Molecular Complexes; Weber, A., Ed.; Springer Netherlands: Dordrecht, 1987; pp 23–42.
- (28) Block, P. A.; Miller, R. E. Near infrared spectroscopy of the HCN-HX (X = Cl, Br, and I) binary complexes. *J. Mol. Spectrosc.* **1991**, *147*, 359–369.
- (29) Fowler, P.; Legon, A.; Peebles, S. Rotational spectrum of HCN···HI and a comparison of properties in the series HCN···HX (X = F, Cl, Br, I and CN). *Chem. Phys. Lett.* **1994**, 226, 501–508.
- (30) Wugt Larsen, R.; Hegelund, F.; Nelander, B. Observation and rovibrational analysis of the ν_2 band of HCN-H³⁵Cl. *Chem. Phys.* **2005**, 310, 163–167.
- (31) Wugt Larsen, R.; Hegelund, F.; Nelander, B. Observation and rovibrational analysis of the intermolecular HCl libration band ν_6^1 of HCN–HCl, DCN–HCl and H¹³CN–HCl. *Phys. Chem. Chem. Phys.* **2005**, 7, 1953–1959.
- (32) Hinchliffe, A. Hydrogen bonding in HCN···HF, HCN···HCl, CH₃CN···HF and CH₃CN···HCl; an ab initio SCF-MO study. *Adv. Mol. Relax. Int. Pr.* **1981**, *19*, 227–237.
- (33) Buckingham, A. D.; Fowler, P. A model for the geometries of van der Waals complexes. *Can. J. Chem.* **1985**, *63*, 2018–2025.
- (34) Buckingham, A.; Fowler, P. Electrostatic models of hydrogen-bonded dimers: a donor-acceptor scale for hydrogen halides and pseudohalides. *J. Mol. Struct.* **1988**, *189*, 203–210.
- (35) Bacskay, G. B.; Kerdraon, D. I.; Hush, N. S. Quantum chemical study of the HCl molecule and its binary complexes with CO, C₂H₂, C₂H₄, PH₃, H₂S, HCN, H₂O and NH₃: Hydrogen bonding and its effect on the ³⁵Cl nuclear quadrupole coupling constant. *Chem. Phys.* **1990**, *144*, 53–69.
- (36) Bacskay, G. B. Hydrogen bonded complexes of HCl with CO, C₂H₂, C₂H₄, PH₃, H₂S, HCN, H₂O and NH₃: Correlated quantum chemical calculations of geometries, energetics, vibrational frequencies and ³⁵Cl quadrupole coupling constants. *Mol. Phys.* **1992**, *77*, 61–73.
- (37) Del Bene, J. E. Hydrogen bonding: Methodology and applications to complexes of HF and HCl with HCN and CH₃CN. *Int. J. Quantum Chem.* **1992**, 44, 527–541.
- (38) Del Bene, J. E.; Person, W. B.; Szczepaniak, K. Properties of Hydrogen-Bonded Complexes Obtained from the B3LYP Functional with 6-31G(d,p) and 6-31+G(d,p) Basis Sets: Comparison with MP2/6-31+G(d,p) Results and Experimental Data. *J. Phys. Chem.* **1995**, 99, 10705–10707.
- (39) García, A.; Cruz, E. M.; Sarasola, C.; Ugalde, J. M. Properties of some weakly bound complexes obtained with various density functionals. *J. Mol. Struct. (Theochem)* **1997**, 397, 191–197.
- (40) Araújo, R. C.; Ramos, M. N. An Ab Initio MP2 Study of HCN-HX Hydrogen Bonded Complexes. *J. Braz. Chem. Soc.* **1998**, *9*, 499–505.
- (41) Del Bene, J. E.; Perera, S. A.; Bartlett, R. J. Hydrogen Bond Types, Binding Energies, and ¹H NMR Chemical Shifts. *J. Phys. Chem.* A **1999**, *103*, 8121–8124.
- (42) George, W. O.; Jones, B. F.; Lewis, R.; Price, J. M. Computations of medium strength hydrogen bonds-complexes of mono- and bi-functional carbonyl and nitrile compounds with hydrogen chloride. *Phys. Chem. Chem. Phys.* **2000**, *2*, 4910–4917.
- (43) Mandal, P. K.; Arunan, E. Hydrogen bond radii for the hydrogen halides and van der Waals radius of hydrogen. *J. Chem. Phys.* **2001**, *114*, 3880–3882.
- (44) van der Avoird, A.; Bondo Pedersen, T.; Dhont, G. S. F.; Fernandez, B.; Koch, H. Ab initio potential-energy surface and rovibrational states of the HCN–HCl complex. *J. Chem. Phys.* **2006**, 124, 204315.
- (45) Ebrahimi, A.; Roohi, H.; Habibi, M.; Hasannejad, M. Determination of gas-phase nucleophilicities and electrophilicities using B···HX bond critical point properties of AIM analysis. *Chem. Phys.* **2006**, 327, 368–372.
- (46) Raghavendra, B.; Mandal, P. K.; Arunan, E. Ab initio and AIM theoretical analysis of hydrogen-bond radius of HD (D = F, Cl, Br, CN, HO, HS and CCH) donors and some acceptors. *Phys. Chem. Chem. Phys.* **2006**, *8*, 5276–5286.

- (47) Domagała, M.lg.; Grabowski, S. J. $X-H\cdots\pi$ and $X-H\cdots N$ hydrogen bonds Acetylene and hydrogen cyanide as proton acceptors. *Chem. Phys.* **2009**, 363, 42–48.
- (48) Gronowski, M.; Kolos, R.; Sadlej, J. Structure, Energetics, and Infrared Spectra of Weakly Bound $HC_{2n+1}N\cdots HCl$ Complexes. A Theoretical Study. J. Phys. Chem. A **2012**, 116, 5665–5673.
- (49) Legon, A. C. A reduced radial potential energy function for the halogen bond and the hydrogen bond in complexes B···XY and B··· HX, where X and Y are halogen atoms. *Phys. Chem. Chem. Phys.* **2014**, *16*, 12415–12421.
- (50) Alkorta, I.; Legon, A. C. Nucleophilicities of Lewis Bases B and Electrophilicities of Lewis Acids A Determined from the Dissociation Energies of Complexes B···A Involving Hydrogen Bonds, Tetrel Bonds, Pnictogen Bonds, Chalcogen Bonds and Halogen Bonds. *Molecules* **2017**, 22, 1786.
- (51) Viana, M. A. A.; Araújo, R. C. M. U.; Neto, J. A. M.; Chame, H. C.; Pereira, A. M.; Oliveira, B. G. The interaction strengths and spectroscopy parameters of the $C_2H_2\cdots HX$ and $HCN\cdots HX$ complexes (X = F, Cl, CN, and CCH) and related ternary systems valued by fluxes of charge densities: QTAIM, CCFO, and NBO calculations. *J. Mol. Model.* **2017**, 23, 1–15.
- (52) McDowell, S. A. Proton acceptor response in hydrogen-bonded XH···WZ (X = F, Cl, Br, FAr, FKr, NC, FCC; WZ = CO, FH, N_2) complexes. *Chem. Phys. Lett.* **2019**, 724, 110–114.
- (53) Cavallo, G.; Metrangolo, P.; Milani, R.; Pilati, T.; Priimagi, A.; Resnati, G.; Terraneo, G. The Halogen Bond. *Chem. Rev.* **2016**, *116*, 2478–2601.
- (54) Kozuch, S.; Martin, J. M. L. Halogen Bonds: Benchmarks and Theoretical Analysis. J. Chem. Theory Comput. 2013, 9, 1918–1931.
- (55) Anderson, L. N.; Aquino, F. W.; Raeber, A. E.; Chen, X.; Wong, B. M. Halogen Bonding Interactions: Revised Benchmarks and a New Assessment of Exchange vs Dispersion. *J. Chem. Theory Comput.* **2018**, 14, 180–190.
- (56) Medved', M.; Iglesias-Reguant, A.; Reis, H.; Góra, R. W.; Luis, J. M.; Zaleśny, R. Partitioning of interaction-induced nonlinear optical properties of molecular complexes. II. Halogen-bonded systems. *Phys. Chem. Chem. Phys.* **2020**, *22*, 4225–4234.
- (57) Aakeröy, C. B.; Fasulo, M.; Schultheiss, N.; Desper, J.; Moore, C. Structural Competition between Hydrogen Bonds and Halogen Bonds. *J. Am. Chem. Soc.* **2007**, *129*, 13772–13773.
- (58) Wolters, L. P.; Bickelhaupt, F. M. Halogen Bonding versus Hydrogen Bonding: A Molecular Orbital Perspective. *ChemistryOpen* **2012**, *I*, 96–105.
- (59) Scheiner, S., Ed. Noncovalent Forces; Springer: Cham, Switzerland, 2015.
- (60) Robertson, C. C.; Wright, J. S.; Carrington, E. J.; Perutz, R. N.; Hunter, C. A.; Brammer, L. Hydrogen bonding vs. halogen bonding: the solvent decides. *Chem. Sci.* **2017**, *8*, 5392–5398.
- (61) Gamekkanda, J. C.; Sinha, A. S.; Desper, J.; Đakovic, M.; Aakeroy, C. B. Competition between hydrogen bonds and halogen bonds: a structural study. *New J. Chem.* **2018**, *42*, 10539–10547.
- (62) Quiñonero, D.; Frontera, A. Hydrogen Bond versus Halogen Bond in HXO_n (X = F, Cl, Br, and I) Complexes with Lewis Bases. *Inorganics* **2019**, 7, 9.
- (63) Riel, A. M. S.; Rowe, R. K.; Ho, E. N.; Carlsson, A. C.; Rappé, A. K.; Berryman, O. B.; Ho, P. S. Hydrogen Bond Enhanced Halogen Bonds: A Synergistic Interaction in Chemistry and Biochemistry. *Acc. Chem. Res.* **2019**, *52*, 2870–2880.
- (64) Møller, C.; Plesset, M. S. Note on an Approximation Treatment for Many Electron Systems. *Phys. Rev.* **1934**, *46*, 618.
- (65) Čížek, J. On the Correlation Problem in Atomic and Molecular Systems. Calculation of Wavefunction Components in Ursell-Type Expansion Using Quantum-Field Theoretical Methods. *J. Chem. Phys.* **1966**, 45, 4256–4266.
- (66) Purvis, G.; Bartlett, R. A full coupled-cluster singles and doubles model: The inclusion of disconnected triples. *J. Chem. Phys.* **1982**, *76*, 1910.

- (67) Raghavachari, K.; Trucks, G. W.; Pople, J. A.; Head-Gordon, M. A fifth-order perturbation comparison of electron correlation. *Chem. Phys. Lett.* **1989**, *157*, 479–483.
- (68) Dunning, T. H. Gaussian basis sets for use in correlated molecular calculations. I. The atoms boron through neon and hydrogen. *J. Chem. Phys.* **1989**, *90*, 1007–1023.
- (69) Kendall, R. A.; Dunning, T. H.; Harrison, R. J. Electron affinities of the first-row atoms revisited Systematic basis sets and wave function. *J. Chem. Phys.* **1992**, *96*, 6796–6806.
- (70) Woon, D. E.; Dunning, T. H. Gaussian basis sets for use in correlated molecular calculations. III. The atoms aluminum through argon. *J. Chem. Phys.* **1993**, *98*, 1358–1371.
- (71) Peterson, K. A.; Woon, D. E.; Dunning, T. H. Benchmark calculations with correlated molecular wave functions. IV. The classical barrier height of the $H+H_2\rightarrow H_2+H$ reaction. *J. Chem. Phys.* **1994**, 100, 7410–7415.
- (72) Wilson, A. K.; Woon, D. E.; Peterson, K. A.; Dunning, T. H. Gaussian basis sets for use in correlated molecular calculations. IX. The atoms gallium through krypton. *J. Chem. Phys.* **1999**, *110*, 7667–7676.
- (73) Peterson, K. A.; Figgen, D.; Goll, E.; Stoll, H.; Dolg, M. Systematically convergent basis sets with relativistic pseudopotentials. II. Small-core pseudopotentials and correlation consistent basis sets for the post-d group 16âÁŚ18 elements. *J. Chem. Phys.* **2003**, *119*, 11113–11123.
- (74) Peterson, K. A.; Shepler, B. C.; Figgen, D.; Stoll, H. On the Spectroscopic and Thermochemical Properties of ClO, BrO, IO, and Their Anions. *J. Phys. Chem. A* **2006**, *110*, 13877–13883.
- (75) Frisch, M. J.; Trucks, G. W.; Schlegel, H. B.; Scuseria, G. E.; Robb, M. A.; Cheeseman, J. R.; Scalmani, G.; Barone, V.; Peterson, G. A.; Nakatsuji, H. et al. *Gaussian16*, revision C.01; Gaussian Inc.: Wallingford, CT, 2016.
- (76) Stanton, J. F.; Gauss, J.; Cheng, L.; Harding, M. E.; Matthews, D. A.; Szalay, P. G. CFOUR, Coupled-Cluster techniques for Computational Chemistry, a quantum-chemical program package, with contributions from A.A. Auer, R.J. Bartlett, U. Benedikt, C. Berger, D.E. Bernholdt, Y.J. Bomble, L. Cheng, O. Christiansen, M. Heckert, O. Heun, C. Huber, T.-C. Jagau, D. Jonsson, J. Jusélius, K. Klein, W.J. Lauderdale, D.A. Matthews, T. Metzroth, L.A. Mück, D.P. O'Neill, D.R. Price, E. Prochnow, K. Ruud, F. Schiffmann, W. Schwalbach, S. Stopkowicz, A. Tajti, J. Vázquez, F. Wang, and J.D. Watts and the integral packages MOLECULE (J. Almlöf and P.R. Taylor), PROPS (P.R. Taylor), ABACUS (T. Helgaker, H.J. Aa. Jensen, P. Jørgensen, and J. Olsen), and ECP routines by A. V. Mitin and C. van Wüllen. For the current version see http://www.cfour.de.
- (77) Kestner, N. R. He-He Interaction in the SCF-MO Approximation. J. Chem. Phys. 1968, 48, 252–257.
- (78) Liu, B.; McLean, A. D. Accurate calculation of the attractive interaction of two ground state helium atoms. *J. Chem. Phys.* **1973**, *59*, 4557–4558.
- (79) Jansen, H. B.; Ros, P. Non-empirical molecular orbital calculations on the protonation of carbon monoxide. *Chem. Phys. Lett.* **1969**, *3*, 140–143.
- (80) Boys, S. F.; Bernardi, F. The calculation of small molecular interactions by the differences of separate total energies. Some procedures with reduced errors. *Mol. Phys.* **1970**, *19*, 553–566.
- (81) Simon, S.; Duran, M.; Dannenberg, J. J. How does basis set superposition error change the potential surfaces for hydrogenbonded dimers? *J. Chem. Phys.* **1996**, *105*, 11024–11031.
- (82) Tschumper, G. S. Reliable Electronic Structure Computations for Weak Non-Covalent Interactions in Clusters. *Rev. Comput. Chem.* **2009**, *26*, 39–90.
- (83) Lu, Y.; Zou, J.; Yu, Q.; Jiang, Y.; Zhao, W. Ab initio investigation of halogen bonding interactions involving fluorine as an electron acceptor. *Chem. Phys. Lett.* **2007**, 449, 6–10.
- (84) Politzer, P.; Murray, J. S.; Concha, M. C. Halogen bonding and the design of new materials: organic bromides, chlorides and perhaps even fluorides as donors. *J. Mol. Model.* **2007**, *13*, 643–650.

- (85) Murray, J. S.; Politzer, P. Molecular Surfaces, van der Waals Radii and Electrostatic Potentials in Relation to Noncovalent Interactions. Croat. Chem. Acta 2009, 82, 267-275.
- (86) Eskandari, K.; Lesani, M. Does Fluorine Participate in Halogen Bonding? Chem.—Eur. J. 2015, 21, 4739-4746.
- (87) Koohi, A. M.; Mahdavifar, Z.; Noorizadeh, S. Can Fluorine form Halogen Bond? Investigation of Halogen Bonds through Steric Charge. ChemistrySelect 2017, 2, 2713-2717.
- (88) Scheiner, S. F-Halogen Bond: Conditions for Its Existence. J. Phys. Chem. A 2020, 124, 7290-7299.
- (89) Saito, K.; Torii, H. Hidden Halogen-Bonding Ability of Fluorine Manifesting in the Hydrogen-Bond Configurations of Hydrogen Fluoride. J. Phys. Chem. B 2021, 125, 11742-11750.
- (90) Hattig, C.; Schmitz, G.; Koßmann, J. Auxiliary basis sets for density-fitted correlated wavefunction calculations: weighted corevalence and ECP basis sets for post-d elements. Phys. Chem. Chem. Phys. 2012, 14, 6549-6555.

TRECOMMENDED Recommended by ACS

Electrostatics, Charge Transfer, and the Nature of the Halide-Water Hydrogen Bond

John M. Herbert and Kevin Carter-Fenk

IANIJARY 27 2021

THE JOURNAL OF PHYSICAL CHEMISTRY A

READ **Z**

Characterization of Type I and II Interactions between **Halogen Atoms**

Steve Scheiner.

MARCH 16, 2022

CRYSTAL GROWTH & DESIGN

READ 🗹

Unconventional Type III Halogen···Halogen Interactions: A Quantum Mechanical Elucidation of σ-Hole···σ-Hole and Di-σ-Hole Interactions

Mahmoud A. A. Ibrahim and Nayra A. M. Moussa

AUGUST 19, 2020

ACS OMEGA

READ **C**

What Types of Noncovalent Bonds Stabilize Dimers $(XCP)_2$, for X = CN, Cl, F, and H?

Janet E. Del Bene, José Elguero, et al.

NOVEMBER 11, 2019

THE JOURNAL OF PHYSICAL CHEMISTRY A

READ **C**

Get More Suggestions >